

Horizontal Wavenumber Spectra Across the Middle Atmosphere From Airborne Lidar Observations During the 2019 Southern Hemispheric SSW

Stefanie Knobloch¹, Bernd Kaifler¹, Andreas Dörnbrack¹, Markus Rapp^{1,2}

¹ German Aerospace Center (DLR), Institute of Physics of the Atmosphere, Oberpfaffenhofen, Germany

² Meteorologisches Institut München, Ludwig-Maximilians-Universität München, Munich, Germany

stefanie.knobloch@dlr.de

INTRODUCTION

- Nastrom and Gage (1983): the horizontal wavenumber spectrum of the troposphere exhibits a power-law behavior of approximately $k^{-5/3}$ on the mesoscales ($2.6 \text{ km} < \lambda < 400 \text{ km}$)
- Previous airborne lidar observations covered only parts of the middle atmosphere (e.g. Kwon et al., 1990, Hostetler et al., 1991, Hostetler et Gardner, 1994, Gao and Meriwether, 1998)
- First observations from 20 km to 80 km altitude by the Airborne Lidar for Middle Atmosphere research (ALIMA) operated during the SouthTRAC-GW campaign September 2019 (Rapp et al., 2021)
- Prevalent theories for the generation of a canonical horizontal spectrum on the mesoscales are stratified turbulence (e.g. Lilly, 1983; Lindborg, 2006; Li and Lindborg, 2018) or interacting Gravity Waves (GWs) (e.g. Dewan, 1979; VanZandt, 1982; Bacmeister et al., 1996)
- A Southern Hemisphere Sudden Stratospheric Warming (SSW) started on 30 August 2019 with a displacement of stratospheric polar vortex towards South America (Fig. 1).
- The critical level for propagating MWs descended to approx. 40 km due to the SSW (Fig. 2).

RESEARCH QUESTIONS

- What is the shape of the horizontal wavenumber spectrum throughout the middle atmosphere in the vicinity of the mountain wave (MW) hotspot above the Southern Andes?
- How is the horizontal wavenumber spectrum in the middle atmosphere affected by GWs and the SSW?

METHOD

- 43 straight flight legs with lengths from 150 km to 2400 km
- Range-corrected photon counts $\gamma(t, z)$ with a resolution of $\Delta t = 1 \text{ min}$ and $\Delta z = 900 \text{ m}$
- Monte-Carlo experiment: photon noise spectra calculated based on $\overline{\gamma(z)}$ and assumption that photon noise follows a Poisson distribution
- Flight leg normalization: $\gamma'(t, z) = \frac{\gamma(t, z)}{\overline{\gamma(z)}}$ (1)
- Power spectral density (PSD): $\text{PSD}_\gamma(k) = |\hat{\gamma}(k)|^2 * \frac{\Delta x^2}{X}$ (2)
- $\lambda_k = k * \Delta x$, $k = [1, 2, \dots, n]$, $k = \frac{2\pi}{\lambda_k}$, $n = \frac{X}{\Delta x}$, $\Delta x = \tau * \overline{GS_{HALO}}$

RESULTS

- Derived horizontal wavelengths range from 22 km to 2000 km (Fig. 3 and 4)
- Below 70 km altitude, most horizontal wavenumber spectra are well above the noise floor (except ST10 due to icing of the laser window; Fig. 3 and 4)
- PSD_γ is reduced by approximately 25 % at $\lambda_k = 200 \text{ km}$ during flights ST09, ST10, ST11, ST12 and ST14 compared to ST08 (Fig. 3)
- Largest values and variability of PSD_γ over the ocean, while on average values larger over land than over the ocean (especially in the mesosphere; Fig. 5)

CONCLUSIONS

- Averaged horizontal wavenumber spectra are statistically robust, rather smooth and exhibit slopes close to $k^{-5/3}$ in stratosphere; slopes deviate from $k^{-5/3}$ for $\lambda_k < 200 \text{ km}$ in the mesosphere
- Influences by horizontally and vertically propagating MWs and potentially non-orographic GWs apparent
- The SSW caused an attenuation of spectral power

Learn more by reading the publication

Altitude dependent horizontal wavenumber spectra changing for the different research flights

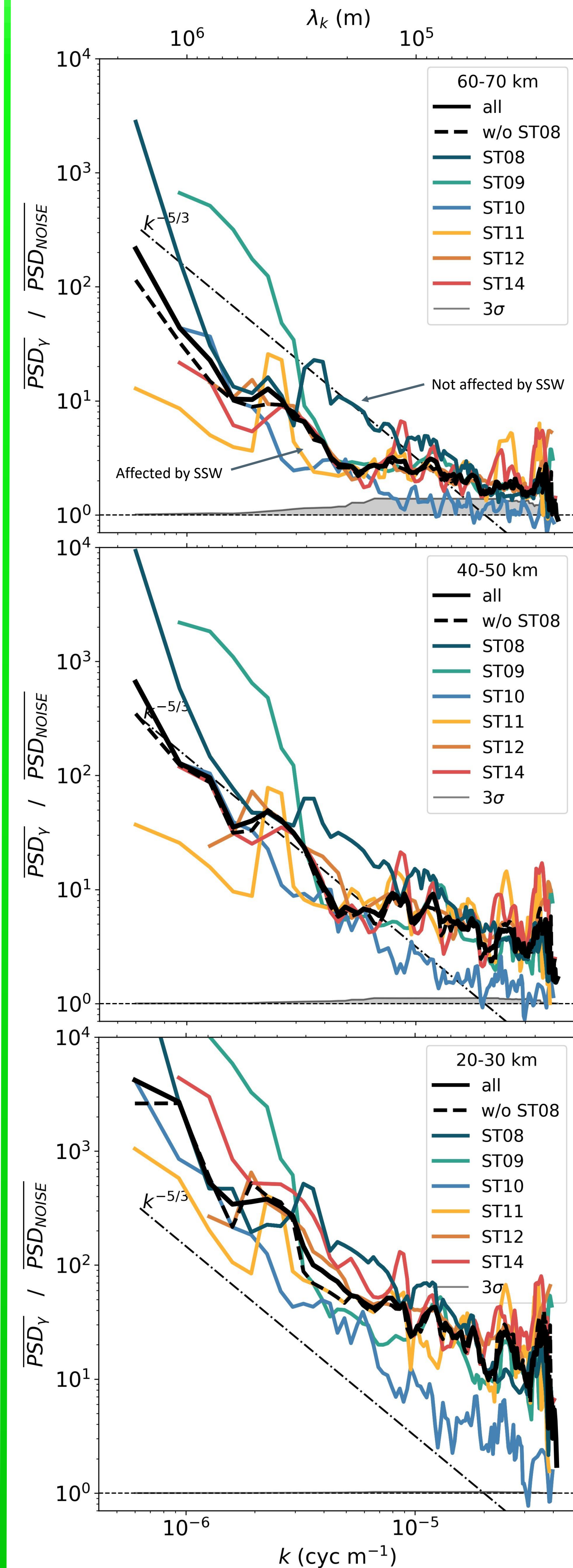


Figure 1: Vertically averaged horizontal wavenumber spectra of all research flights.



OUTLOOK

Further development: extention of ALIMA by an iron resonance channel for lower thermosphere and wind measurements
Future application: e.g. ALIMA observations during strong stratospheric polar vortex conditions, investigation of horizontal GW propagation

Atmospheric Conditions and Mountain wave propagation during the SSW

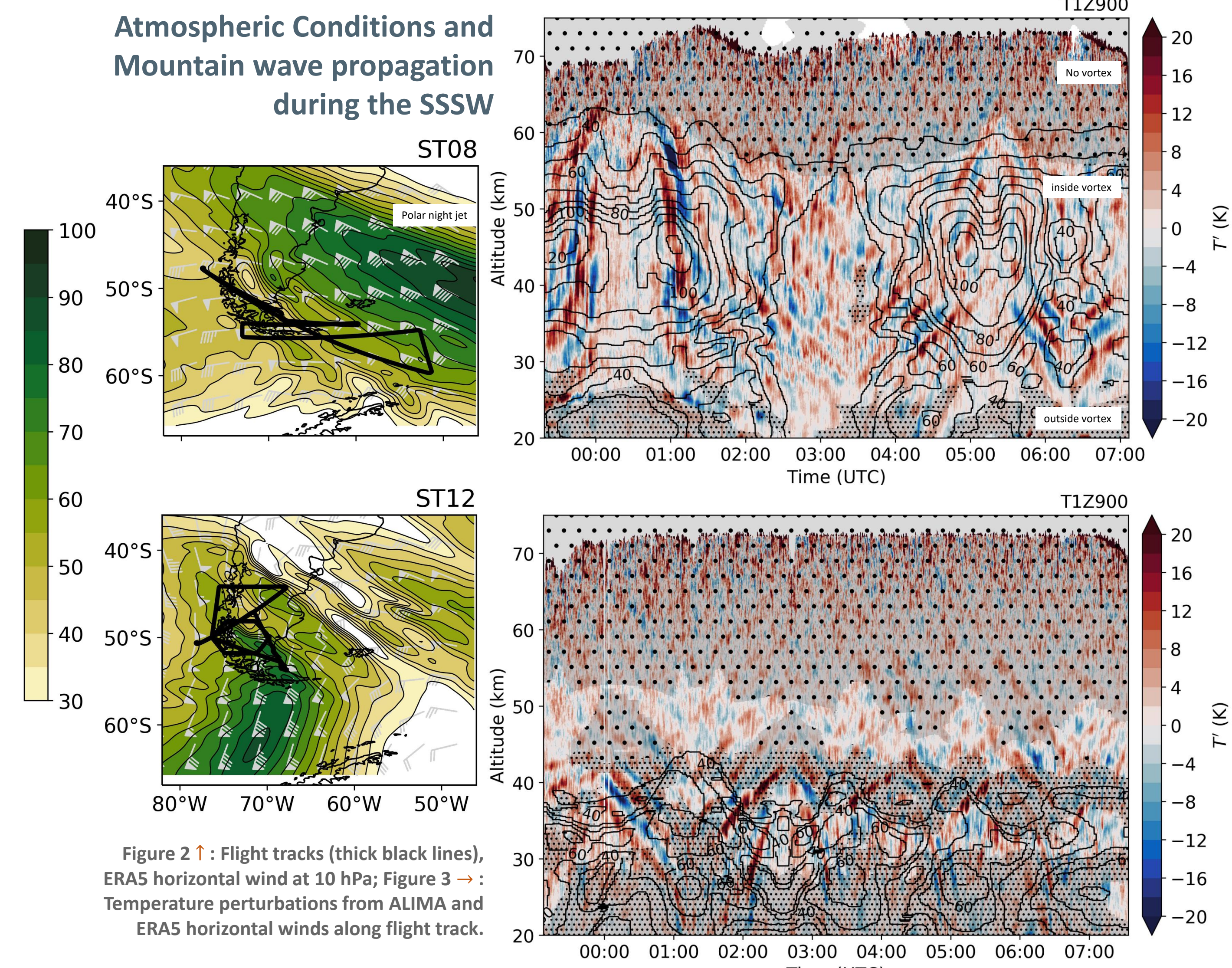
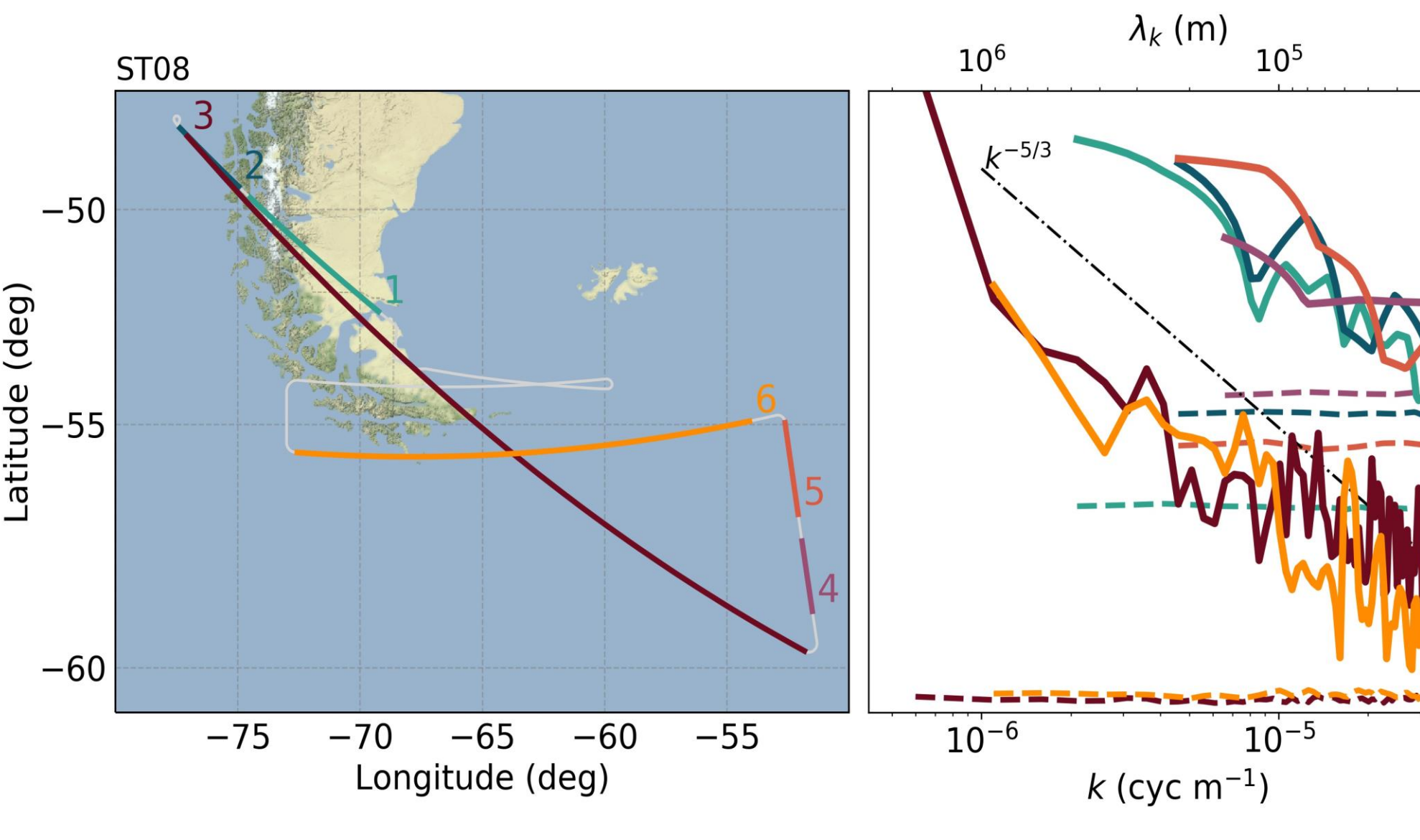


Figure 2: Flight tracks (thick black lines), ERA5 horizontal wind at 10 hPa; Figure 3: Temperature perturbations from ALIMA and ERA5 horizontal winds along flight track.



Individual horizontal wavenumber spectra of ST08 close to $k^{-5/3}$
Figure 4: Flight legs of ST08; Photon noise spectra (colored dashed lines).

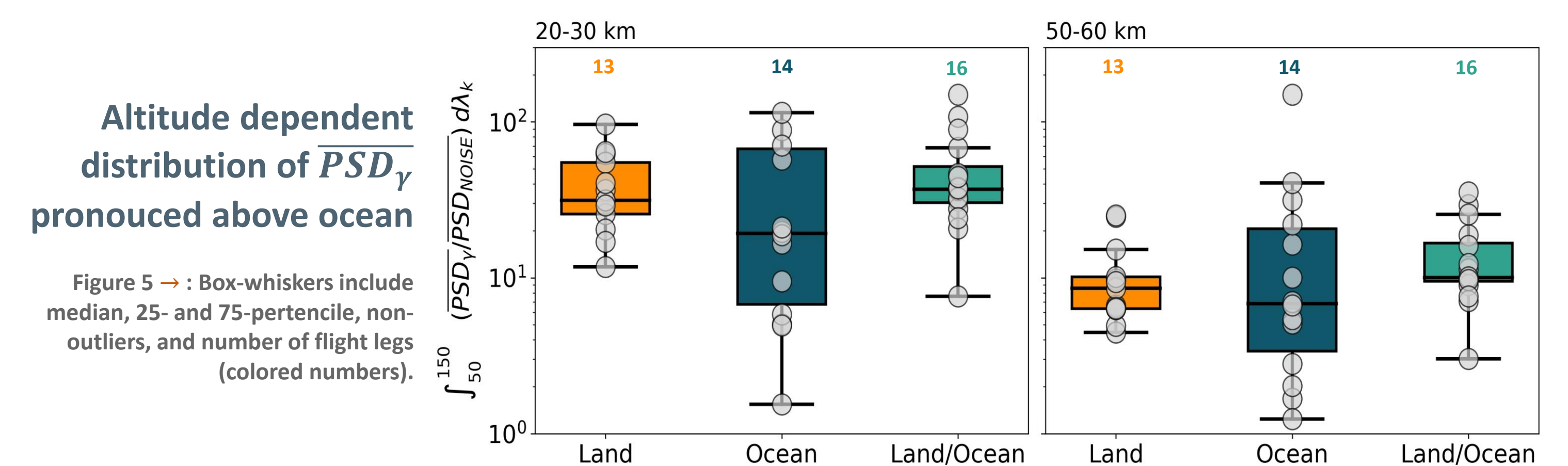


Figure 5: Box-whiskers include median, 25- and 75-percentile, non-outliers, and number of flight legs (colored numbers).

REFERENCES

- Baumgardner, J. F., S. D. Eckermann, P. A. Newman, L. Lutz, K. R. Chan, M. H. Proffitt, and B. L. Gary (1990), "Stratospheric horizontal wavenumber spectra of winds, potential temperature, and atmospheric tracers observed by high-altitude aircraft", *JGR: Atmospheres* 101, D5, pp. 9461–9470, doi:<https://doi.org/10.1029/90JD00385>
- Gao, X., and C. S. Meriwether (1998), "Mesoscale airborne in situ and lidar observations of variance and spatial structure in the troposphere and stratosphere regions", *JGR: Atmospheres* 103, D6, pp. 6391–6396, doi:10.1029/97JD03080
- Dewan, F. M. (1979), "Stratospheric Wave Spectra Resembling Turbulence", In: *Science* 204, 4395, pp. 832–835, doi:10.1126/science.204.4395.832
- Gao, X., and C. S. Meriwether (1998), "Mesoscale airborne in situ and lidar observations of variance and spatial structure in the troposphere and stratosphere regions", *JGR: Atmospheres* 103, D6, pp. 6391–6396, doi:10.1029/97JD03080
- Hostetler, C. A., C. S. Gardner, R. A. Vincent, and D. Lescler (1991), "Spectra of gravity wave density and wind perturbations observed during ALOHA-90 on the 25 March flight between Maui and Christmas Island", In: *GRL* 18, 7, pp. 1325–1328, doi:10.1029/91GL01150
- Hostetler, C. A., and C. S. Gardner (1994), "Observations of horizontal and vertical wave number spectra of gravity wave motions in the stratosphere and mesosphere over the mid-Pacific", In: *JGR: Atmospheres* 99, D1, pp. 1283–1302, doi:10.1029/93JD00297
- Knobloch, S., B. Kaifler, A. Dörnbrack, and M. Rapp (2023), "Horizontal Wavenumber Spectra Across the Middle Atmosphere From Airborne Lidar Observations During the 2019 Southern Hemispheric SSW", *GRL*, 50, 14, e2023GL104357, doi:10.1029/2023GL104357
- Kwon, K. H., D. C. Smit, and C. S. Gardner (1990), "Airborne sodium lidar observations of horizontal and vertical wave number spectra of mesopause density and wind perturbations", In: *JGR: Atmospheres* 95, D9, pp. 13723–13736, doi:10.1029/JD095iD09p13723
- Li, Q., and E. Lindborg (2018), "Weakly or Strongly Mesoscale Dynamics Close to the Tropopause?", *JAS* 75, 4, pp. 1212–1229, doi:10.1175/JAS-D-17-0063.1
- Lilly, D. K. (1983), "Stratified Turbulence and the Mesoscale Variability of the Atmosphere", *JAS*, 40, 3, pp. 749–761, doi:10.1175/1520-0469(1983)040<0749:STMTMA>2.0.CO;2
- Lindborg, E. (2006), "The energy cascade in a strongly stratified fluid", In: *Journal of Fluid Mechanics* 550, pp. 207–242, doi:10.1017/S0022112005008128
- Nastrom, G. D., and D. C. Gage (1985), "A Climatology of Atmospheric Wave Spectra of Wind and Temperature Observed by Commercial Aircraft", *JAS*, 42, 9, pp. 950–960, doi:10.1175/1520-0469(1985)042<0950:ACAWOS>2.0.CO;2
- Rapp, M., B. Kaifler, A. Dörnbrack, S. Gisinger, T. Mixo, R. Reichert, N. Wildemann, A. Giez, L. Krasauskas, P. Preuse, R. Eckert, M. Gellenhus, R. Reichert, M. Rapp, W. Woiwode, F. Friedl-Vallon, B.-M. Sinnhuber, A. de la Torre, P. Alexander, J. L. Hormaechea, D. Janches, M. Garhammer, J. L. Chau, F. Conte, P. Hoer, and A. Engel (2021), "SOUTHTRAC-GW: An Airborne Field Campaign to Explore Gravity Wave Dynamics at the World's Strongest Hotspot", *BAMS*, 102, 4, E871–E893, doi:10.1175/BAMS-D-20-0034.1
- VanZandt, T. E. (1982), "A universal spectrum of buoyancy waves in the atmosphere", *GRL*, 9, 5, pp. 575–578, doi:10.1029/GL009i005p00575